Kinetic modelling and simulation of bioanode and biocathode in a bioelectrochemical cell for carbon dioxide reduction

Vafa Ahmadi. Nabin Aryal
Department of Process, Energy and Environmental Technology, University of South-Eastern Norway, Porsgrunn, Norway (E-mail: vafa.ahmadi@usn.no, nabin.aryal@usn.no)

Abstract: Bioelectrochemical systems (BESs) have garnered extensive research attention for their biosynthesis and environmental remediation applications. One of the challenges to upscaling BES for carbon dioxide (CO_2) methanation is energy-efficient process development. Investigations are ongoing to determine the relationship between the yield of electroactive microorganisms, the key candidates for electrochemical reactions with external electricity input. Consequently, simulating processes, particularly with biocathode for biosynthesis and bioanode for remediation, gives crucial insights for designing efficient BESs. The framework for establishing Nernst-Monod equations for modelling BES, starts from bioanode, where anode respiring bacteria (ARB) oxidate organic carbon compounds to CO_2, and generate the proton (H^+). In this work, kinetic modelling was applied to calculate the biomass yield of ARBs corresponding to the applied anodic voltage. The generated CO_2 and H^+ from the anode determined the biomass yield of electroactive methanogens and acetogens on the cathode. Two biofilm models were established for anodic and cathodic biofilm growth in Aquasim simulation tool. Results showed that the concentration of organic carbon compound (acetate) available for ARB, had a significant impact on the biofilm thickness and biomass concentration on the biofilm, especially at + 0.3 V. The optimum anode voltage which released the highest CO_2 and H^+, was + 0.3 V. The anodic and cathodic biofilm thickness reached respectively 3 mm and 55 µm at + 0.3V and 10 $g.L^{-1}$ acetate input to the anode chamber. Moreover, methanogens surpassed acetogens on the biocathode for CO_2 reduction to methane rather than acetate. In addition, acetate consumption rate by ARB at anode was remarkably faster than acetate production at cathode.

Keywords: Carbon dioxide, Anode respiring bacteria, Methanogens, Acetogens, Biocathode, Bioanode, Methane and Acetate.

1. INTRODUCTION

Biomethane production from anaerobic digestion (AD) is one of the strong alternatives to fossil fuels. However, AD may face limitations due to multiple process-related factors, in particular high pH fluctuation, low productivity, or inhibition effect due to volatile fatty acids (VFA). Understanding the limitations of the process and the factors affecting microbial growth is essential for increasing biomethane production. Bioelectrochemical systems (BESs) are one of the emerging technologies that benefit from biofilms with electroactive microbes that consume electricity. BES is a promising technology to overcome the limitations of AD process. The electricity input aids the microbes and enhances the breakdown of organic matter. Meanwhile, it can stop unwanted side reactions which limit production. Therefore, the purity of target products such as methane (CH_4), acetic acid or other valuable organic carbon compounds can be increased (Aryal et al., 2020). The methods currently available for the electrochemical reduction of CO_2 need external overpotentials due to high energy demand, to overcome ohmic losses. If enough electric potential is provided, bacteria and archaea can overcome potential losses in BES, where CO_2 can be reduced to valuable energy carriers such as CH_4 or other biochemicals (Rittmann and McCarty 2020).

The anode potential (oxidation voltage) can be correlated with the metabolic activities of biocatalysts and the corresponding energy dissipation. In microbial electrochemical cells (MECs), the applied electricity can help microorganisms obtain electromotive forces for better growth and maintenance(Torres et al., 2008). In MEC, a dense biofilm on anode oxidizes the organic and inorganic molecules if enough energy is available (Rabaey and Verstraete, 2005). The external energy supports and enhances the microbial community of anode- oxidizing bacteria (ARB) due to the microbial selectivity process. Besides, the activity of methanogenic microbial biomass at cathode will be enhanced. Autotrophic methanogens will become more abundant in the biofilm matrix, and a mixture of autotrophic and heterotrophic microbial biomass communities will also increase in the suspended media of the reactor.

Generally, direct electron transfer (DET) or mediated electron transfer is well accepted when abiotic electrodes and electroactive microbes interact with each other. In mediated electron transfer theories, the kinetics of electron transfer starts from ARB. These bacteria oxidize organic compounds, which

provide electrons for cathode. ARBs transfer electrons to the anode via anodic respiration. Like methanogens, ARBs have a constrained range of electron donors. The most popular and beneficial electron donor by far is acetate. Certain ARBs can also use hydrogen (H_2), formate, ethanol, propionate, glucose, and other sugars as electron donors. Anode respiration is a novel and distinct kind of catabolism. A general electron donor is used, but the electron acceptor is substituted with a solid acceptor, completing the catabolic reaction. *Geobacter sulfurreducens* and *Shewanella* species are the two most well-known ARBs. However, it is yet unclear how ARBs accomplish extracellular electron transfer (EET) biochemically (Rittmann and McCarty 2020).

BES reactor configuration can be divided into multi-chamber and single-chamber reactors. In dual chamber reactors, the anode and cathode are separated by an ion exchange membrane, preventing possible anodic/cathodic reversible reactions. However, in membrane-less single-chamber reactors, the anode and cathode are in the same chamber (Aryal et al., 2022). Therefore, in the mixed microbial environment of the reactor, it is possible that an organic matter, such as acetate, is oxidized at the anode via electrochemical reactions or by ARB, and then reproduced at cathode by acetogenic microbes (May et al., 2016; Yates et al., 2017). The oxidation of acetate by ARBs at the anode can be faster than the reproduction of acetate at the cathode. Additionally, the competition between methanogens and acetogens in the cathode chamber is another important area of study. In dual-chamber reactors, it is possible to measure the acetate consumption rate by ARBs and the acetate production rate by autotrophic acetogens. The half-reaction of acetate oxidation (R.1) shows that acetate is oxidized to CO_2, HCO_3^-, and H^+ (Rittmann and McCarty 2020):

$$\frac{1}{8}CH_3COO^- + \frac{3}{8}H_2O \rightarrow \frac{1}{8}CO_2 + \frac{1}{8}HCO_3^- + H^+ + e^- \quad E^0_{ox} = +0.28\ \text{V} \quad \text{(R.1)}$$

The reproduction of acetate can occur at the cathode via (R.2).

$$2CO_2 + 8H^+ + 8e^- \rightarrow CH_3COO^- + 2H_2O \qquad E^0_{red} = -0.284\ \text{V} \quad \text{(R.2)}$$

Methanogens at the cathode produce CH_4 via (R.3) through the DET mechanism:

$$CO_2 + 8H^+ + 8e^- \rightarrow CH_4 + 2H_2O \qquad E^0_{red} = -0.248\ \text{V} \quad \text{(R.3)}$$

This work simulates ARB growth based on acetate consumption at different anodic voltages. The H^+ and CO_2 released from acetate oxidation by electroactive ARBs will be used to calculate the growth of cathodic biofilm by autotrophic methanogenic species for CH_4 production. Furthermore, the reproduction of acetate by acetogenic species has been studied to compare the acetate consumption rate with the acetate reproduction rate.

2. METHODOLOGY

The electron acceptor of the ARBs has no concentration because it is a solid anode. Microorganisms are considered in direct contact with the electrode (Rittmann and McCarty 2020). ARBs utilize the electron donor molecules, which in this work is acetate. The activity of the electroactive cathodic biofilm is limited by the number of electrons and H^+ flowing to the cathode for CH_4 and acetate production (Fig. 1). The process scheme involves wastewater containing acetate and biomass flowing to the anode with 1 day hydraulic retention time (HRT) (Ahmadi and Dinamarca, 2022). Additionally, biomass-containing wastewater enters the cathode chamber with 1 day HRT. In the BES reactor illustrated in Fig. 1, voltage is applied to the anode. The anode potential creates an electron pull on the cathode, which absorbs the electrons flowing from bioanode to the biocathode.

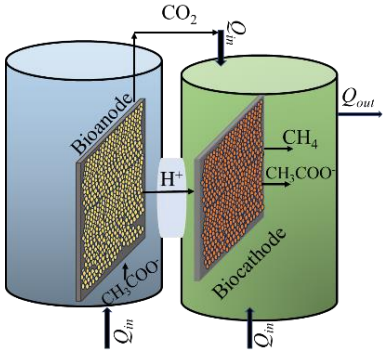

Fig. 1. Schematic diagram of the CO_2 reduction with a dual-chamber BES reactor separated by ion exchange membrane. The ARB bioanode oxidizes acetate. Then H^+ and CO_2 flow to biocathode for CH_4 and acetate production.

In a BES, the anode acts as the electron acceptor instead of an organic electron acceptor. The cathode serves as the electron donor instead of an organic electron donor. Therefore, it can be hypothesized that in a BES system, two complete biological redox reactions take place, as illustrated in Fig. 2.

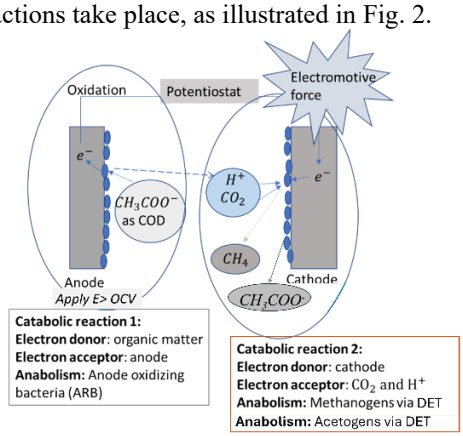

Fig. 2. Graphical view of catabolism and anabolism in a BES reactor. Anabolism refers to cell growth, while catabolism refers to product formation. OCV is the open circuit voltage of anode; any voltage higher than this will be relatively positive.

2.1 *Simulation parameters and inputs*

Tab. 1 provides all the parameters, expressions, and inputs for simulating the model. The biomass formula is considered to be $CH_{1.8}O_{0.5}N_{0.2}$ (Heijnen and Kleerebezem, 1999). Aquasim version 2.1 (Reichert, 1998) was used to simulate the kinetics of the bioanode and biocathode for CO_2 reduction. Furthermore, the acetate input (S_{ac}) to the anode chamber is assumed to be 1, 5, and 10 $g.L^{-1}$. The molar concentrations of acetate are 16.66, 83.33, and 160.66 $mol.m^{-3}$, respectively. The

CO_2 and H^+ inputs to the cathode are obtained after simulating the anodic biofilm kinetics. Then, the CO_2 and H^+ produced during steady-state anodic oxidation will be used for CH_4 and acetate production at cathode.

2.2 Model assumptions

-The model consists of two biofilms: one for ARB attachment in the anode chamber and the second, the cathodic biofilm (or biocathode), for the formation of methanogenic and acetogenic biofilms.
- The substrate is acetate for organic-oxidizing bacteria, such as *Acetobacter acetae* (ARB1), and sulfate-reducing bacteria (SRB), assumed as ARB2, that grow on acetic acid (Tremblay et al., 2019).
- The substrates for biocathode are CO_2 and H^+ from acetate oxidation at the anode. *Sporomusa ovata* can be considered as acetogens, and *methanobacterium* as methanogens on the cathode (Zhang et al., 2017).
- pH is considered 7 and the pressure is 1 atm.
- CO_2 and HCO_3^- are in equilibrium, so the input to the cathode is considered to be CO_2.
- The biofilm decay is accounted by considering a detachment velocity in the system.
- BES oxidation and reduction are specifically emphasized.
- No electrons are lost in other reactions, and potential losses in the system are ignored.
- The impact of electrode material and the self-potential of the electrodes are not considered.

2.3 Model expressions

The simulation in this work started at the anode, where ARBs oxidize the chemical oxygen demand (COD) as acetate. The Nernst-Monod equation is used to calculate the ARB biomass growth rate ($\frac{d[X_{ARB}]}{dt}$) and the variation in the concentration of acetate ($\frac{d[S_{ac}]}{dt}$), as well as the produced CO_2 and H^+. Equations 1 and 2 illustrate the anodic model expressions (Korth et al. 2015; Fischer 2017; Rittmann and McCarty 2020).

$$\frac{d[X_{ARB}]}{dt} = X_{ARB} \cdot \left(\mu_{X_{ARB}}^{max} \cdot \emptyset_{an} \cdot \frac{S_{ac}}{K_{S_{ac}} + S_{ac}} \cdot \frac{1}{1 + exp\left|-(E_{app} - E_{KA})\frac{F}{RT}\right|} - k_{d,ac} \right) \quad (1)$$

$$\frac{d[S_{ac}]}{dt} = -\left(\frac{d[X_{ac}]}{dt}\right) / Y_{ac} \quad (2)$$

Where X_{ARB} is the ARB biomass concentration, $\mu_{X_{ARB}}^{max}$ is the maximum growth rate of ARB, $\emptyset_{an}$ is the fraction of electroactive biomass in the biofilm, assumed 0.75, S_{ac} is the acetate molar concentration, $K_{S_{ac}}$ is the half-saturation constant of acetate, E_{app} is the applied voltage, E_{KA} is the potential at which the biomass growth rate is half of its maximum, $k_{d,ac}$ is the ARB decay rate, F is the Faraday constant (96485.3 C. mol^{-1}), R is the universal gas constant (8.314 J. mol^{-1}. K^{-1}), T is temperature (K), and Y_{ac} is the ARB biomass yield based on acetate consumption. All the terms with values are given fully in Tab.1.

In R1, the Nernst term is a critical factor for the electroactive biomass growth. Every electrode material has a natural voltage relative to its surrounding electrolyte, known as the open circuit voltage (OCV).

Table 1. Model parameters for the simulation

Parameter, unit	Value	Ref
Diffusivity of acetate, $m^2 \cdot d^{-1}$	$9.41 \cdot 10^{-5}$	(Ahmadi and Dinamarca, 2022)
Diffusivity of CH_4, $m^2 \cdot d^{-1}$	$1.296 \cdot 10^{-4}$	(Ahmadi and Dinamarca, 2022)
Diffusivity of CO_2, $m^2 \cdot d^{-1}$	$1.658 \cdot 10^{-4}$	(Ahmadi and Dinamarca, 2022)
Diffusivity of H^+, $m^2 \cdot d^{-1}$	$8.04 \cdot 10^{-5}$	(Ahmadi and Dinamarca, 2022)
Diffusivity of biomass, $m^2 \cdot d^{-1}$	$1 \cdot 10^{-7}$	(Ahmadi and Dinamarca, 2022)
Biomass density, $mol \cdot m^{-3}$	220	(Ahmadi and Dinamarca, 2022)
Half saturation concentration of CO_2, $mol \cdot m^{-3}$	3.8	(Eddy et al., 2014)
Half saturation concentration of H^+, $mol \cdot m^{-3}$	0.0002	(Eddy et al., 2014)
Half saturation concentration of acetate, $mol \cdot m^{-3}$	0.03	(Eddy et al., 2014)
Max growth rate of ARB1, d^{-1}	12	Assumed
Max growth rate of ARB2, d^{-1}	2.4	Assumed
Max growth rate of methanogens, d^{-1}	2.28	Assumed
Max growth rate of acetogens, d^{-1}	1.008	Assumed
Acetogenic growth yield	0.02	Assumed
Methanogenic growth yield	0.083	Assumed
ARB1 growth yield	0.0384	Assumed
ARB2 growth yield	0.28	Assumed
Initial biofilm thickness, m	$1 \cdot 10^{-10}$	This work
Half maximum growth voltage of ARB1, V	-0.2	(Heijnen and Kleerebezem, 1999)
Half maximum growth voltage of ARB2, V	-0.1	(Heijnen and Kleerebezem, 1999)
Inflow, $m^3 \cdot d^{-1}$	0.1	This work
Biofilm reactor volume, m^3	0.1	This work
Biofilm surface area, m^2	10	This work
Anode voltage, V	-0.2, -0.1, 0.3	This work
Acetic acid concentration, $mol \cdot m^{-3}$	16.66, 83.33, 166.6	This work
CO_2 concentration, $mol \cdot m^{-3}$	Simulation results	This work
H^+ concentration, $mol \cdot m^{-3}$	Simulation results	This work

An applied voltage higher than OCV increases oxidation on the electrode. Therefore, the applied voltage in this work is relatively voltage with respect to OCV. The OCV of the anode is crucial in determining the applied voltage and the potential range within which E_{kA} falls.

Figure 3 shows the calculated Nernst term with respect to the anodic voltage. According to Rittmann and McCarty (2020), when E_{KA} is higher, more voltage is required to reach the

maximum Nernst term of 1. Thus, lower E_{kA} is more advantageous for the BES in terms of energy savings.

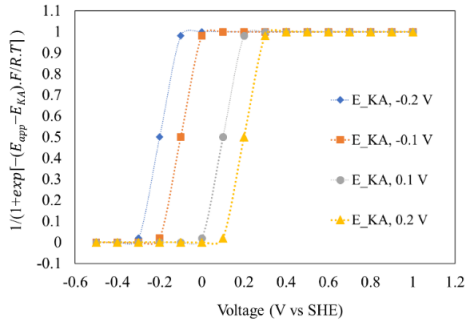

Fig. 3. Variation of the Nernst term with respect to the anode voltage at different E_{KA} values, ranging from -0.2 to +0.2 V.

The dynamic current generation ($\frac{dj}{dt}$, A.m^{-2}) via ARB biomass on anode (current density, A·m^{-2}) can be obtained by (6) (Torres et al., 2008).

$$\frac{dj}{dt} = \frac{d[X_{ARB}]}{dt} \cdot \gamma \cdot L_f \cdot (f_s^0 - 1) \quad (6)$$

where, γ represents the equal electron production, which is 8 for acetate oxidation. L_f is the biofilm thickness (m). The term f_s^0 refers to electron equivalent cell synthesis coefficient, which can be obtained by thermodynamic equations as fully described by Rittmann and McCarty (2020). At lower voltage, f_s^0 is reduced. At higher voltage, f_s^0 increases leading to a higher biomass population on the anode. This concept is explained in a thermodynamic evaluation of biomass growth with respect to the voltage (Ahmadi and Aryal, 2024).

In BES, voltage is applied either to either the anode or cathode. This creates a potential difference between electrodes, enabling redox reactions. Therefore, to establish the methanogenic and acetogenic biomass growth rates on the cathode ($\frac{d[X_{CH_4}]}{dt}$ and $\frac{d[X_{ac}]}{dt}$, respectively), using the multiplicative Monod equation without the Nernst term is a more reasonable approach, as shown in equations (3), (4), and (5). The number of electrons and H^+ from acetate oxidation is equal. Thus, when H^+ is available, it indicates that enough electrons have been delivered to undergo CO_2 reduction (Korth et al. 2015; Fischer 2017; Rittmann and McCarty 2020).

$$\frac{d[X_{CH_4}]}{dt} = X_{CH_4} \cdot \left(\mu_{X_{CH_4}}^{max} \cdot \emptyset_{cat} \cdot \frac{S_{CO_2}}{K_{CO_2}+S_{CO_2}} \cdot \frac{S_{H^+}}{K_{H^+}+S_{H^+}} - k_{d,CH_4}\right) \quad (3)$$

$$\frac{d[X_{ac}]}{dt} = X_{ac} \cdot \left(\mu_{X_{ac}}^{max} \cdot \emptyset_{cat} \cdot \frac{S_{CO_2}}{K_{CO_2}+S_{CO_2}} \cdot \frac{S_{H^+}}{K_{H^+}+S_{H^+}} - k_{d,ac}\right) \quad (4)$$

$$\frac{d[S_{CH_4}]}{dt} = \left(\frac{d[X_{CH_4}]}{dt}\right)/Y_{CH_4} \quad (5)$$

where X_{CH_4} is the methanogenic biomass content, $\mu_{X_{CH_4}}^{max}$ is the maximum growth rate of methanogens, $\emptyset_{cat}$ is the fraction of electroactive biomass on cathode, S_{CO_2} is the molar concentration of CO_2, K_{CO_2} is the half-saturation constant of CO_2, S_{H^+} is the molar concentration of H^+, K_{H^+} is the half-saturation constant of H^+, k_{d,CH_4} is the decay rate of methanogens, X_{ac} is the acetogenic biomass content, $\mu_{X_{ac}}^{max}$ is the maximum growth rate of acetogens, $k_{d,ac}$ is the decay rate of acetogens, $\frac{d[S_{CH_4}]}{dt}$ is the methane production rate in molar concentration, Y_{CH_4} is the methanogenic biomass yield based on CO_2 and H^+ consumption.

3. RESULTS AND DISCUSSION

3.1 Concentration profiles at anode

Figure 4 shows the total acetate consumption by ARBs in the anode chamber at different concentrations. The concentration profiles show the relation between the anodic voltage and acetate consumption. When the anode voltage is equal to E_{kA} of ARB, the growth rate of ARB is half of its maximum value. As a result, it takes approximately 17 days for ARB to consume all the acetate. By increasing the voltage to -0.1 V, acetate consumption accelerates, with all the acetate being consumed after 5 days. An even higher anodic voltage results in faster acetate consumption, completely depleting the acetate in 2 days. At higher acetate concentrations, the consumption profile follows the same order, but it takes longer to deplete the total acetate at -0.2 V. However, increasing the voltage helps reduce the acetate depletion time at higher concentrations.

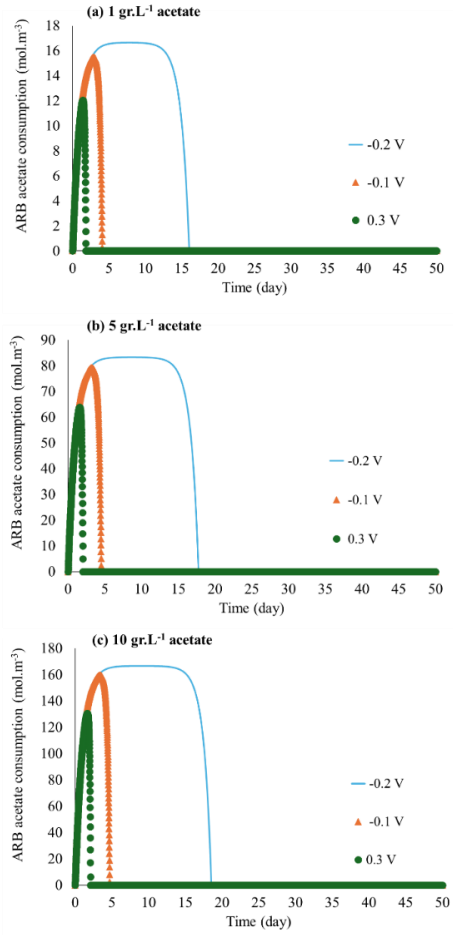

Fig. 4. Acetate consumption by ARB biofilm for different acetate concentration in anode chamber. The applied anode voltage is -0.2, -0.1 and +0.3 V.

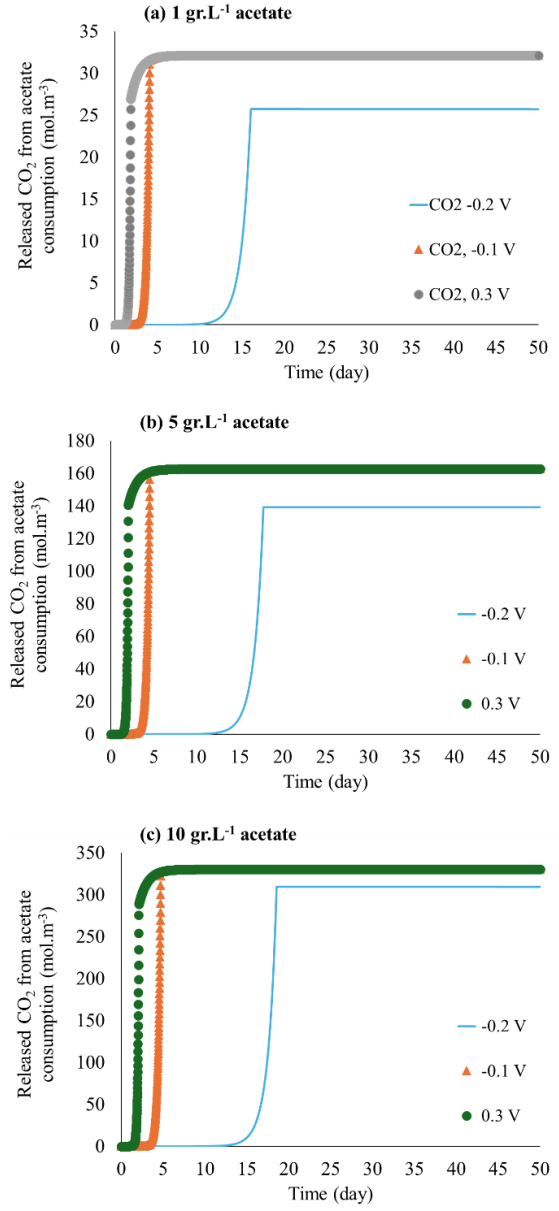

Fig. 5. The released CO_2 from ARB oxidation of acetate. The applied anode voltage is -0.2, -0.1 and +0.3 V.

The correspondence concentration profiles of CO_2 (Fig. 5) and H^+ (Fig. 6) reflects the same trend as at higher concentration of acetate, higher amount of CO_2 and H^+ will be released that will flow to cathode to be consumed by acetogens and methanogens. Also, the graphs show that higher anode voltage helps shortening the H^+ evolution.

The ARB biofilm thickness (Fig. 7) at anode is more dependent on the availability of substrate for the ARB than the applied voltage at anode. Nevertheless, +0.3 V significantly increases the biofilm thickness to 3 mm while at -0.2 V, the biofilm thickness will be 1.5 mm where the applied voltage is equal to E_{KA} of one ARB species. At -0.1 V, the thickness reaches 2.2 mm for 10 $g.L^{-1}$ acetate input. The graphs show that at low substrate concentration, the effect of voltage on the biofilm thickness is not significant. For 1 $g.L^{-1}$ acetate input, the biofilm thickness will be 55, 57, 59 µm at -0.2 V, -0.1 V and +0.3V respectively. For 5 $g.L^{-1}$ acetate input, the biofilm thickness reaches 110, 117 and 121 µm correspondingly for -0.2, -01 and +0.3 V.

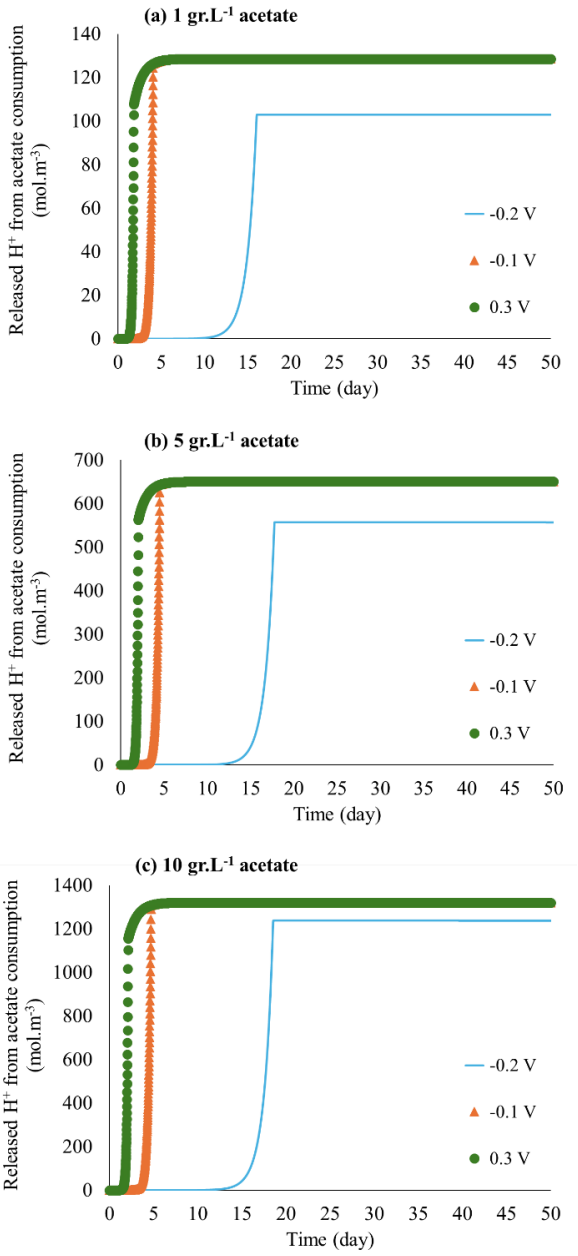

Fig. 6. The released H^+ from ARB oxidation of acetate. The applied anode voltage is -0.2, -0.1 and +0.3 V.

Since 10 $g.L^{-1}$ acetate input to anode resulted in the highest biofilm thickness, the ARB biomass concentration (Fig. 8) is provided for different voltages and 10 $g.L^{-1}$ acetate concentration. Here in Fig. 8 also, 10 $g.L^{-1}$ acetate input at higher voltage of 0.3 V, increases the biomass concentration on anode. The reason is the Nernst term in Eq.1 will be equal to 1 which gives the highest biomass concentration.

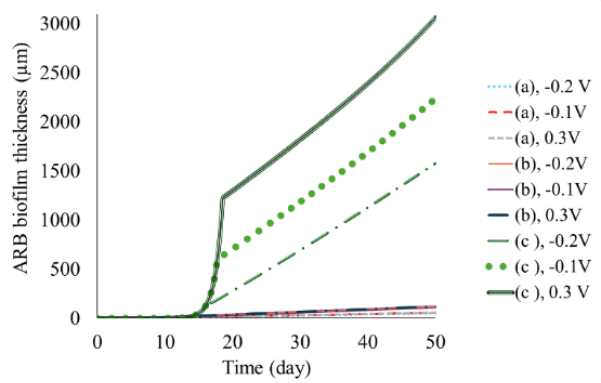

Fig. 7. ARB biofilm thickness at different acetate concentrations; (a) 1 g.L^{-1}, (b) 5 g.L^{-1}, (c) 10 g.L^{-1} acetate at bioanode. The applied anode voltage is -0.2, -0.1 and +0.3 V.

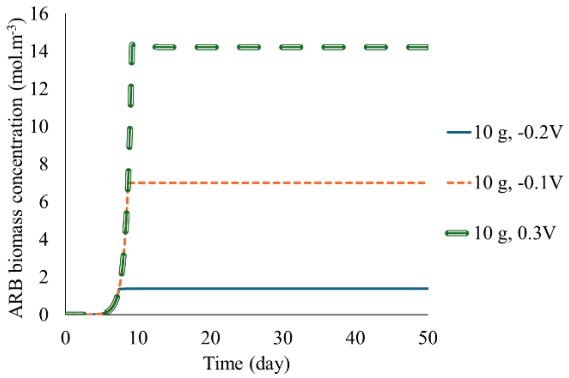

Fig. 8. The anode respiring bacteria (ARB) concentration at -0.2, -0.1, and 0.3V for 10 g.L^{-1} acetate input.

In the current density plots in Fig. 9, the bioelectrochemical current density which can be generated directly by the ARB, is the highest at +0.3V when the acetate input is 10 g.L^{-1} in the anode chamber. The biomass concentration is also higher (Fig. 8); therefore, microbes can break down more substrate to electrons, CO_2 and H^+. Also, in a bioanode, at the start of the biofilm formation, the current density is very low in the micro ampere levels, and after day 10, when the biomass starts to form significantly, the current density increases faster. These simulation results fit the experimental observations in other research work. The bioelectrochemical current density is low at the starting days and increases over time as a dense biofilm is formed on the electrode surface (Li et al., 2020). Moreover, Figure 9 indicates clearly that increasing the applied voltage to BES will not increase the bioelectrochemical current density if not enough substrate is available for bio-oxidation. This is one of the problems which happens in experimental research that high voltage at a low organic matter liquid, leads to many problems such as electrode failure, or the electron generation will not be mainly due to the oxidation of organic matter. In these conditions, increasing the voltage leads to the electrochemical oxidation of the buffer compounds, ammonium, salts, minerals, or water (Sivalingam et al., 2020; Wagner et al., 2010)

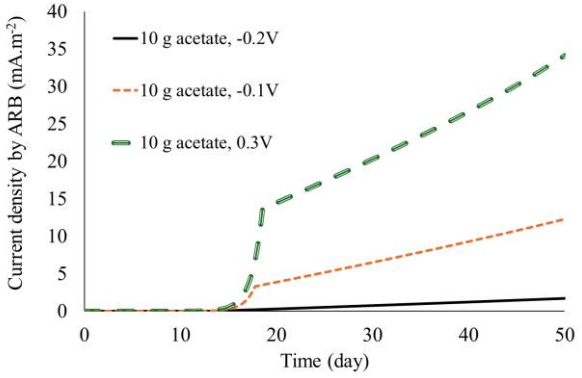

Fig. 9. Current generation by ARB from acetate consumption at 0.3V anode voltage.

3.2. Concentration profiles at cathode

The corresponding CO_2 consumption profiles via biocathode is presented in Fig. 10. The profiles show that the amount of CO_2 consumed by the cathodic biofilm significantly depends on the activity of ARB. In addition to the dependence on the applied anodic voltage and acetate concentration in the anodic chamber, the methanogens and acetogens on the biofilm need more days before the biofilm gets saturated by CO_2 and H^+, and afterwards, CH_4 and acetate production starts. Here, is the illustration of the reason for lag phase in BES reactors to reach stable and maximum CH_4 production. The H^+ consumption profile is also presented in Fig. 11. In the CO_2 and H^+ profiles, it is depicted that the availability of H^+ and CO_2 for cathode, depends both on the applied voltage and acetate concentration. So, lack of organic matter in the anode chamber can be a more significant reason than the applied voltage. Also, the profiles shift with respect to the applied voltage again shows that at higher anode voltage, the CO_2 and H^+ will be available faster for the cathodic microbes. Therefore, the biocathode becomes stable faster at +0.3 V vs SHE compared to lower voltage.

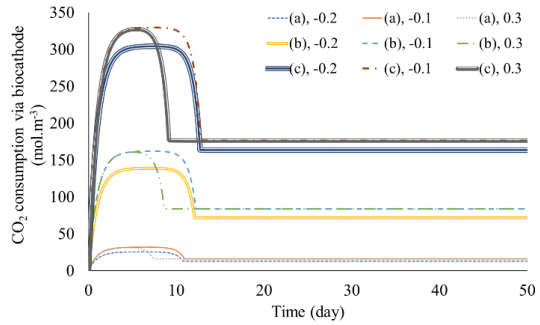

Fig. 10. CO_2 consumption via biocathode, in case of (a) 1 g.L^{-1}, (b) 5 g.L^{-1} and (c) 10 g.L^{-1} acetate for bioanode. The applied anode voltage is -0.2, -0.1 and +0.3 V.

In the H^+ consumption profiles in Fig. 11, the H^+ will be completely consumed by the biocathode while CO_2 remains in the system. This is because according to the acetate oxidation reaction, two moles CO_2 and eight moles H^+ will be available in case of assuming all the CO_2 and H^+ will be available for Doieight moles H^+. That is why a part of the CO_2 will remain unconsumed. For consumption of more CO_2, H^+ should be provided at a higher voltage from other sources such as water, phosphate, sulphate, or ammonium (Rabaey et al., 2009).

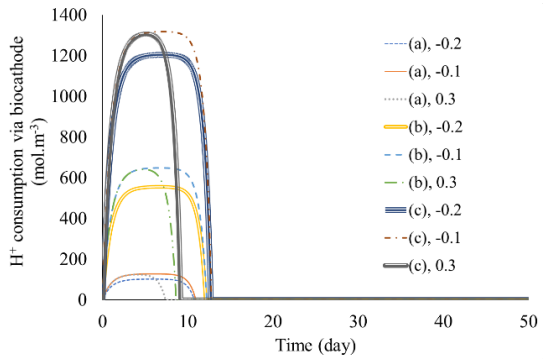

Fig. 11. H+ consumption via biocathode, in case of (a) 1 g.L^{-1}, (b) 5 g.L^{-1} and (c) 10 g.L^{-1} acetate for bioanode. The applied anode voltage is -0.2, -0.1 and +0.3 V.

CH_4 production profiles in Fig. 12 show that there is a direct relation between the acetate input to anode and the applied anodic voltage with CH_4 production. CH_4 will be higher and faster as a result of 10 g.L^{-1} acetate and +0.3 V applied voltage at anode. It should be noted that +0.3 V is a relative value with respect to the open circuit potential (OCV) of the anode. At +0.3 V at anode, the released CO_2 from oxidation of 10 g.L^{-1} acetate, the amount of CH_4 will be the highest according to the parameters in this work, and CH_4 production starts after 6 days. The startup time of CH_4 production is influenced by the voltage. At all acetate concentrations, +0.3 V at anode, leads to higher H^+ and CO_2 release, which reduces the startup time of the process.

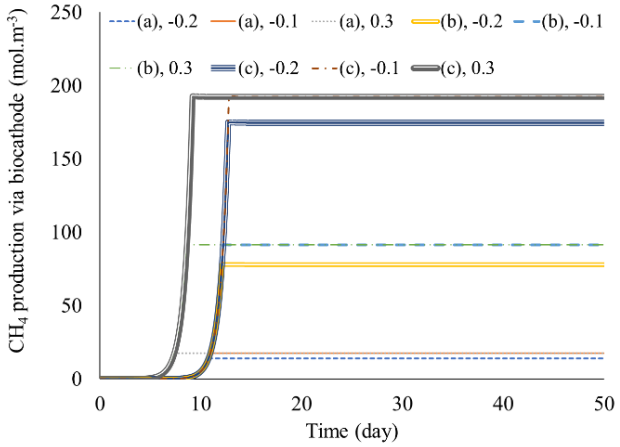

Fig. 12. CH_4 production via biocathode, (a) in case of 1 g.L^{-1} acetate, (b) 5 g.L^{-1} acetate and (c) 10 g.L^{-1} available acetate for bioanode. The applied anode voltage is -0.2, -0.1 V and +0.3.

Figure 13 shows the amount of acetate production in the cathode is very insignificant compared to CH_4 production. Also, acetate production reaches a peak of 0.007 mol.m^{-3}, then it starts to decrease until reaching 0 until day 25. For acetate production, two moles of CO_2 should be consumed. Another reason is the assumed yield and max growth rate of methanogens, which greatly impacts the results. However, in numerous experimental works, CH_4 production surpasses acetate production in a BES reactor.

The results clearly illustrate that acetate oxidation rate in Fig. 4, is much faster than acetate production in Fig. 13. Acetate production is negligible compared to acetate consumption. In many research work, if acetate is the final product, methanogenic inhibitor is used to stop methanogens. Therefore, acetogens will not have competing species, and acetate content will increase in the system (Sivalingam et al., 2022).

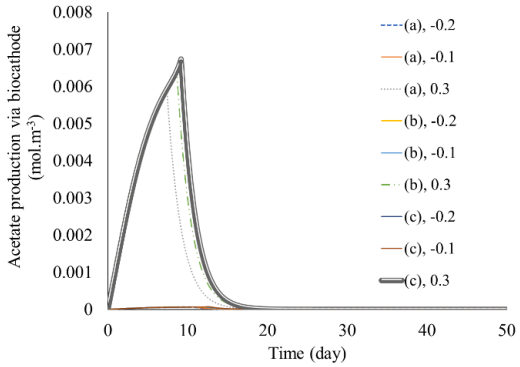

Fig. 13. Acetate production via biocathode, in case of (a) 1 g.L^{1}, (b) 5 g.L^{-1} and (c) 10 g.L^{-1} acetate input to anode. The applied anode voltage is -0.2, -0.1 and +0.3 V.

The cathodic biofilm thickness (Fig. 14) shows that the higher concentration of acetate which is oxidized at anode leads to higher CO_2 and H^+ input to cathode. Therefore, the cathodic biofilm is thicker when the acetate input to anode is 10 g.L^{-1} because it releases higher concentration of CO_2 and H^+. Also, +0.3 V anode voltage led to a thicker biofilm at all concentrations. Also, at +0.3 V anode voltage, the cathodic biofilm starts to grow faster compared to lower voltage. Also, since the growth of autotrophic microbes which grow on inorganic carbon is slower than organic carbon consumption, the ARB biofilm at anode at 10 g.L^{-1} acetate input and +0.3V is 3 mm which is 5 times thicker than the cathodic biofilm 55µm. This is reasonable because organic matter is easier to consume compared to inorganic carbon source (CO_2) for microbes (Abreu et al. 2022; Rittmann and McCarty 2020).

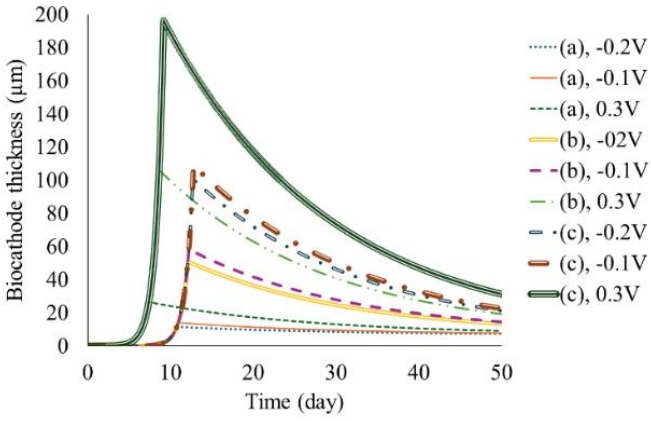

Fig. 14. The cathodic biofilm thickness at different CO_2 and H^+ concentrations resulted from acetate oxidation at anode at -0.2, -0.1 and +0.3 V. (a): 1 g.L^{-1}, (b): 5 g.L^{-1}, (c): 10 g.L^{-1} acetate input to anode.

4. CONCLUSIONS

This simulation work gives a critical insight on the kinetics of bioanode and biocathode in a dual chamber BES reactor. It

should be noted that the model in this work is made according to a single electron donor acetate. In a BES, other sources of electrons and H^+ can take part in oxidation reactions which could be bioelectrochemical or electrochemical. Assessment of the effect of other electron donors on the kinetics of CH_4 production can be considered for further work. The simulation gives a clear vision about the importance of concentration of electron donors and the relation between biomass growth and voltage. Therefore, the simulation will be used for process design and future validation of the results. The kinetic simulation helps regulating the reactor conditions to obtain the optimum biomass on anode and cathode to carry on bioelectrochemical reactions.

REFERENCES

Abreu, A.P., Morais, R.C., Teixeira, J.A., Nunes, J. (2022). A comparison between microalgal autotrophic growth and metabolite accumulation with heterotrophic, mixotrophic and photoheterotrophic cultivation modes. Renewable and Sustainable Energy Reviews 159, 112247. doi. 10.1016/j.rser.2022.112247

Ahmadi, V., Aryal, N. (2024). Evaluation of the relationship between voltage and microbial yield in a bioelectrochemical reactor for optimization of methane production, in: 18th IWA World Conference on Anaerobic Digestion – IWA. IWA, Istanbul.

Ahmadi, V., Dinamarca, C. (2022). Simulation of the Effect of Local Electric Potential and Substrate Concentration on CO2 Reduction via Microbial Electrosynthesis.

Aryal, N., Ghimire, N., Bajracharya, S. (2020). Coupling of microbial electrosynthesis with anaerobic digestion for waste valorization, in: Advances in Bioenergy. Elsevier, pp. 101–127.

Aryal, N., Zhang, Y., Bajracharya, S., Pant, D., Chen, X. (2022). Microbial electrochemical approaches of carbon dioxide utilization for biogas upgrading. Chemosphere 291, 132843.

Eddy, M., Abu-Orf, M., Bowden, G., Burton, F.L., Pfrang, W., Stensel, H.D., Tchobanoglous, G., Tsuchihashi, R., (Firm), A. (2014). *Wastewater engineering: treatment and resource recovery*. McGraw Hill Education.

Fischer, K. (2017). Mathematical modelling of electron transfer modes in electroactive microorganisms.

Heijnen, J.J., Kleerebezem, R. (1999). Bioenergetics of microbial growth. Encyclopedia of bioprocess technology: Fermentation, biocatalysis, and bioseparation 1, 267–291.

Korth, B., Rosa, L.F.M., Harnisch, F., Picioreanu, C. (2015). A framework for modeling electroactive microbial biofilms performing direct electron transfer. Bioelectrochemistry 106, 194–206.

Li, M., Li, Y.-W., Yu, X.-L., Guo, J.-J., Xiang, L., Liu, B.-L., Zhao, H.-M., Xu, M.-Y., Feng, N.-X., Yu, P.-F. (2020). Improved bio-electricity production in bio-electrochemical reactor for wastewater treatment using biomass carbon derived from sludge supported carbon felt anode. Science of the total environment 726, 138573.

May, H.D., Evans, P.J., LaBelle, E. V. (2016). The bioelectrosynthesis of acetate. Curr Opin Biotechnol 42, 225–233.

Rabaey, K., Angenent, L., Schroder, U., Keller, J. (2009). Bioelectrochemical systems. IWA publishing.

Rabaey, K., Verstraete, W. (2005). Microbial fuel cells: novel biotechnology for energy generation. Trends Biotechnol 23, 291–298.

Reichert, P. (1998). Aquasim 2.0-user manual. Swiss Federal Institute for Environmental Science and Technology. Dubendorf, Switzerland.

Rittmann, B.E., McCarty, P.L. (2020). *Environmental Biotechnology: Principles and Applications*, 2nd Edition. ed. McGraw-Hill Education, New York.

Sivalingam, V., Ahmadi, V., Babafemi, O., Dinamarca, C. (2020). Integrating syngas fermentation into a single-cell microbial electrosynthesis (MES) reactor. Catalysts 11, 40.

Sivalingam, V., Winkler, D., Haugen, T., Wentzel, A., Dinamarca, C. (2022). Syngas fermentation and microbial electrosynthesis integration as a single process unit. Bioresour Technol 356, 127314.

Torres, C.I., Marcus, A.K., Parameswaran, P., Rittmann, B.E. (2008). Kinetic Experiments for Evaluating the Nernst−Monod Model for Anode-Respiring Bacteria (ARB) in a Biofilm Anode. Environ Sci Technol 42, 6593–6597. doi. 10.1021/es800970w

Tremblay, P.-L., Faraghiparapari, N., Zhang, T. (2019). Accelerated H2 evolution during microbial electrosynthesis with Sporomusa ovata. Catalysts 9, 166.

Wagner, R.C., Call, D.F., Logan, B.E. (2010). Optimal set anode potentials vary in bioelectrochemical systems. Environ Sci Technol 44, 6036–6041.

Yates, M.D., Ma, L., Sack, J., Golden, J.P., Strycharz-Glaven, S.M., Yates, S.R., Tender, L.M. (2017). Microbial electrochemical energy storage and recovery in a combined electrotrophic and electrogenic biofilm. Environ Sci Technol Lett 4, 374–379.

Zhang, G., Feng, S., Jiao, Y., Lee, D.-J., Xin, Y., Sun, H. (2017). Cathodic reducing bacteria of dual-chambered microbial fuel cell. Int J Hydrogen Energy 42, 27607–27617.